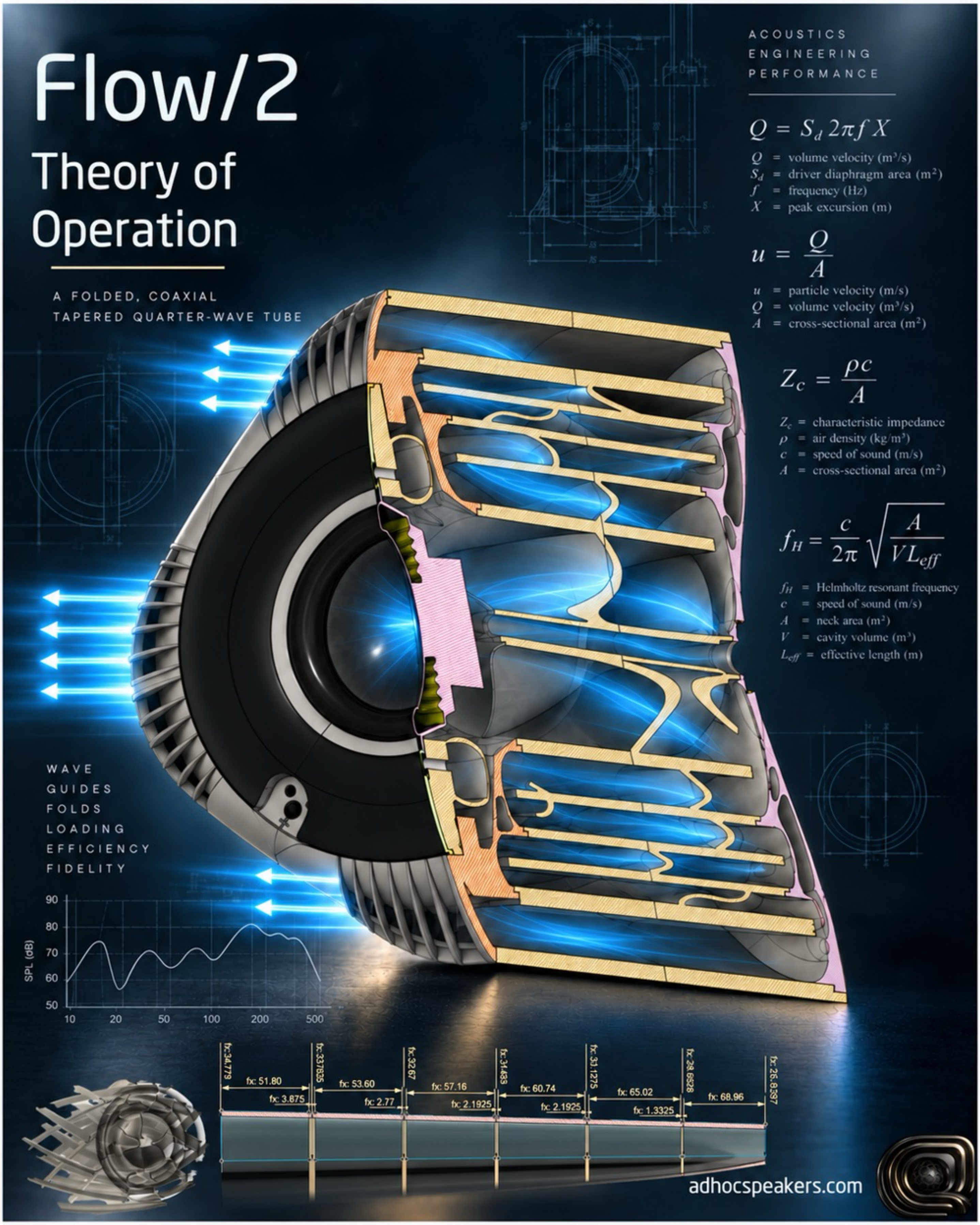

Flow/2
Theory of Operation
A FOLDED, COAXIAL TAPERED QUARTER-WAVE TUBE
ACOUSTICS
ENGINEERING
PERFORMANCE
$Q = S_d 2\pi f X$
Q = volume velocity (m³/s)
S_d = driver diaphragm area (m²)
f = frequency (Hz)
X = peak excursion (m)
$u = \frac{Q}{A}$
u = particle velocity (m/s)
Q = volume velocity (m³/s)
A = cross-sectional area (m²)
$Z_c = \frac{\rho c}{A}$
Z_c = characteristic impedance
ρ = air density (kg/m³)
c = speed of sound (m/s)
A = cross-sectional area (m²)
$f_H = \frac{c}{2\pi}\sqrt{\frac{A}{VL_{eff}}}$
f_H = Helmholtz resonant frequency
c = speed of sound (m/s)
A = neck area (m²)
V = cavity volume (m³)
L_{eff} = effective length (m)
WAVE
GUIDES
FOLDS
LOADING
EFFICIENCY
FIDELITY
SPL (dB)
90
80
70
60
50
10
20
50
100
200
500
fx:34.779
fx: 51.80
fx: 3.875
fx: 53.60
fx: 2.77
fx:32.67
fx: 57.16
fx: 2.1925
fx: 60.74
fx: 2.1925
fx: 65.02
fx: 1.3325
fx: 68.96
adhocspeakers.com

Table of Contents

Figures

Tables

Flow/2 Theory of Operation

The Drive

Flow/2 is a folded, coaxial tapered quarter-wave loudspeaker developed to fit an acoustic line approximately 1.8 meters long into a very small enclosure. This document describes how that geometry evolved and how the finished design manages the acoustic problems created by folding and packaging such a line. It examines the six unequal-length segments, taper, coaxial arrangement, gyroidic vanes, dimples, pimples, clefts, tuned Helmholtz resonators, folds, S5-to-S6 transition, and exit system. It also presents the calculations used to establish line length, modal frequencies, pressure behavior, airflow velocity, fold behavior, resonator placement, and the conditions under which nonlinear airflow may occur. The design goal throughout is useful quarter-wave low-frequency loading from a compact enclosure with internal tube modes, reflections, airflow losses, and audible flow noise kept under control.

I wanted a pair of small, good-sounding speakers to sit beside my computer monitor on the desktop. I also wanted useful bass from a small driver. I thought a tapered quarter-wave tube, or TQWT, might offer a path toward that goal: a long acoustic line whose length supports low-frequency output. I knew the line would need to approach 1.8 meters in length to support the bass range I had in mind. It was 1996.

Fitting a 1.8-meter-long TQWT into a tiny package would bring challenges. There is no magic in acoustics, so compromises seemed inevitable. Or were they? The question was simple: how could I fit a transmission line nearly two meters long into a compact enclosure and still have it sound good?

That question led to a new arrangement. I would divide the line into segments, with each segment forming a ring around the segment nested inside it, all sharing a common axis and connected by folds. I called the concept the Folded Coaxial TQWT, or FCTQWT, and eventually patented the geometry. The patented design describes a continuous transmission line formed by interleaved coaxial tube segments connected through successive folds. By nesting the segments along substantially the same longitudinal axis, the acoustic line occupies a compact enclosure whose depth can be reduced to approximately one-third of the corresponding unfolded transmission-line length (Bouvier, 2011).

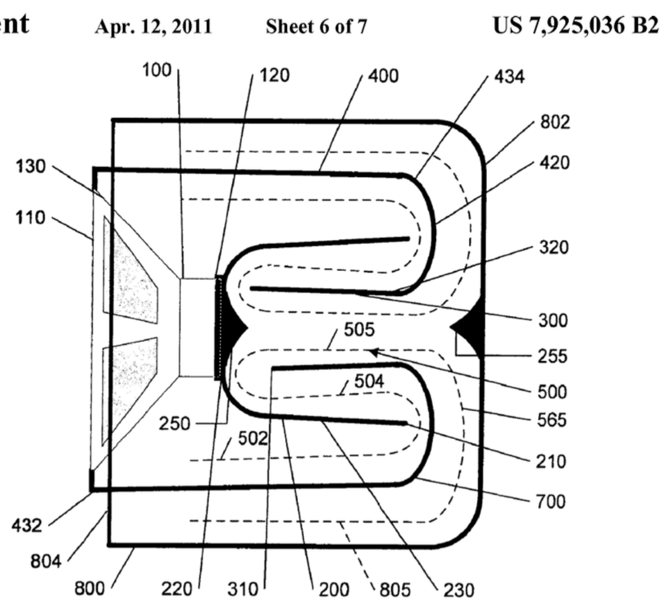

Early folded coaxial transmission-line geometry. From Bouvier, U.S. Patent No. 7,925,036 B2 (2011).

Thirty years of development followed. In 2003, I printed a three-fold tube. In 2010, a four-fold tube followed. In 2020, I printed a six-fold design with a passive resistor behind the driver. I hoped the resistor would attenuate high-frequency energy entering the tube. The resistor failed to produce the desired acoustic result. The work also led me to create a unique linear, symmetric suspension. In 2024, I developed the six-fold version without the resistor.

Six coaxial segments came next, followed by internal vanes. Along the way, I followed DIY loudspeaker groups, 3D-printing groups, and extreme transmission-line loudspeaker groups. I studied Audio Engineering Society publications, papers in the Journal of the Acoustical Society of America, and every other source of audio technology I could find. Those sources gave me many ideas and a deeper understanding of the acoustic and mechanical problems I was trying to solve.

The project continued because, from 2003 onward, each new design could be 3D-printed as a physical prototype. I could hear it, inspect it, measure it, and carry the results into the next design. Each version taught me something about the materials and processes of 3D printing, folded-line geometry, taper, reflections, standing waves, driver loading, and packaging.

In 2025, I added dimples, pimples, and clefts to surfaces and edges within the enclosure. I also replaced the sixth coaxial segment with four corner passages to reduce the enclosure size. Now, in Flow/2, I have added gyroidic vanes and Helmholtz resonators designed to reduce the strongest higher-order tube resonances. Flow/2 is the current form of the design. Printing the enclosure and measuring its acoustic behavior will show how closely it meets the objectives described here. It is where that thirty-year progression has led.

The resulting geometry resolved the packaging problem and defined the engineering work that followed: controlling the acoustic behavior of a long, tapered line folded into six closely spaced passages. Every change in area, direction, wall shape, and internal structure can affect pressure, particle velocity, reflection, and modal behavior. Flow/2 therefore treats the tube itself as part of the acoustic control system.

The following sections describe how its dimensions and internal features were developed to distribute resonances, disturb repeated reflection paths, reduce selected higher-order modes, maintain line-area continuity through the folds, control airflow at high excursion, and deliver the remaining low-frequency energy through the four S6 passages and permanent exit grilles.

Tube Taming Tuning

The first problem was the tube itself. I had planned initially to use DSP equalization to manage the peaks and dips I expected from the transmission line. I had assumed physical control would be difficult, perhaps impossible. Corrective equalization seemed like the practical route. Listening tests changed that view: the required EQ introduced audible artifacts and altered the character of the system. I set that approach aside.

The next possibility was stuffing the line. Stuffing can reduce tube modes. It also dissipates acoustic energy and can reduce low-frequency output when used heavily. I tried many ways to fill the line and treat its walls. Heavy stuffing did reduce the modes, but the resulting loss of low-frequency output defeated the purpose of building Flow/2. Wall lining was difficult to implement and produced little benefit.

That was the turning point. The tube itself had to provide the solution. I took a more scientific approach, treating the line as an engineering system whose behavior could be shaped through its construction. Flow/2 therefore uses unequal segment lengths, taper, coaxial geometry, shaped folds, dimples, pimples, clefts, twisted vanes, and tuned Helmholtz resonators to control the acoustic effects produced by the compact enclosure.

Each method addresses a different part of the problem. The six segment lengths run from 259 to 345 mm; the longest is 33% greater than the shortest. Their unequal lengths are designed to spread the principal longitudinal resonances and reduce the opportunity for reflected waves to coincide and strengthen one another. Taper and coaxial geometry establish the line's basic acoustic structure. Shaped folds, dimples, pimples, clefts, and twisted or gyroidic vanes are designed to redirect and distribute reflected energy. Side-branch Helmholtz resonators are tuned to calculated target regions near 149, 239, 335, and 432 Hz.

Together, these features are designed to lower the modal Q of the targeted modes, a measure of the sharpness and persistence of their resonances, and to reduce the amplitude and sharpness of tube-generated peaks and dips. Preserving the line's low-frequency loading remains a design requirement. Now, Flow/2 uses DSP only for crossover, driver protection, and overall system control; its physical design aims to make DSP correction for tube modes unnecessary.

Geometry

A Folded, Coaxial Tapered Quarter Wave Tube: Compact Packaging Through Coaxial Geometry.

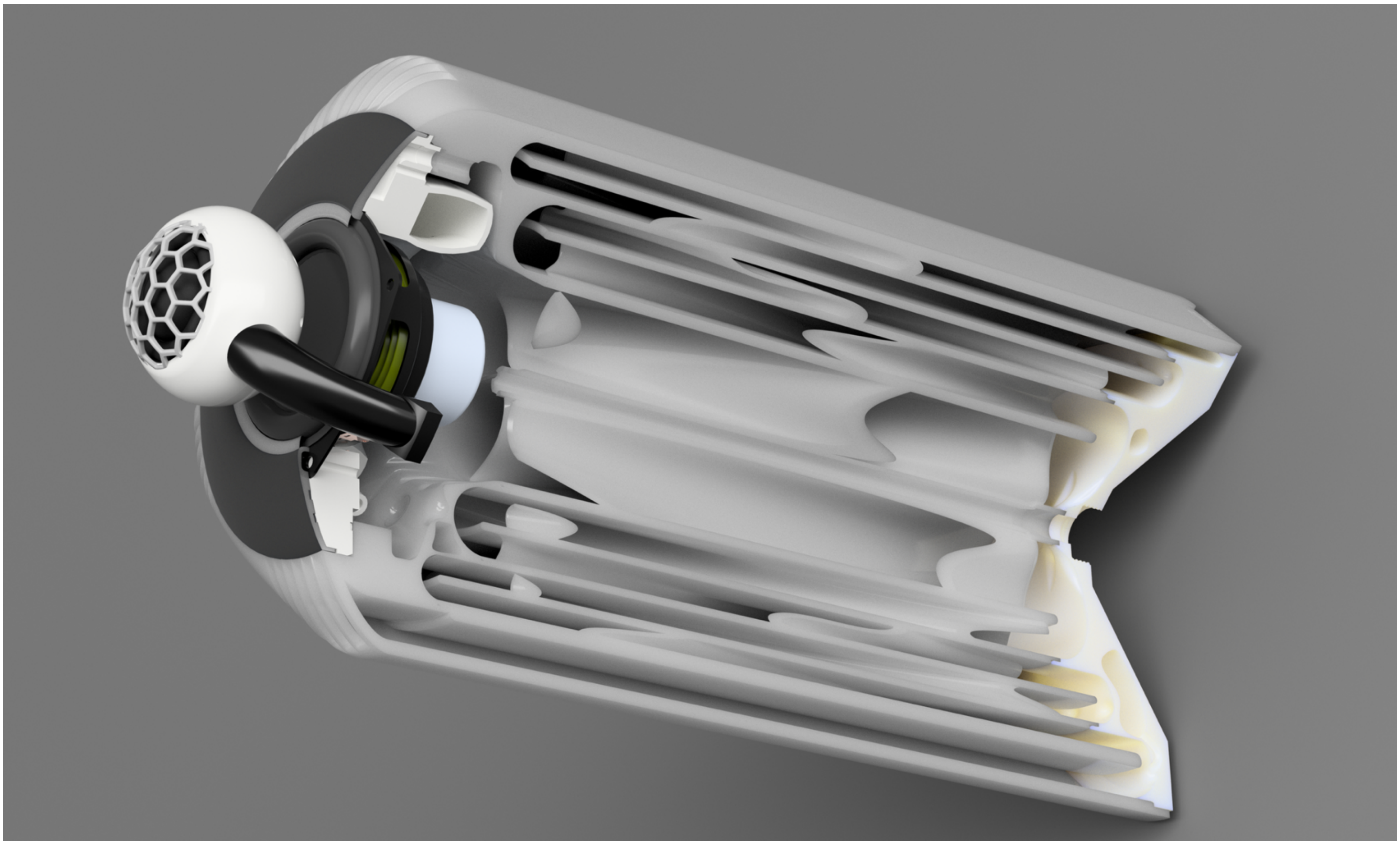

Three-quarter cutaway view of the Flow/2 showing tube segments, folds, gyroidic vanes and Helmholtz Resonator chambers.

Flow/2 is based on a series of folded, coaxially nested ring segments that together form a tapered quarter-wave tube. This document describes the structure of that acoustic line and the methods used to identify, control, and reduce its longitudinal and axial tube modes, standing waves, and reflections.

Additive manufacturing makes this internal geometry practical. Curved resonator throats, irregular cavities, folded passages, recessed surface features, and twisted vanes can be printed directly into the enclosure structure. The resonator chambers use otherwise available volume within the bezel and base, and their throats can reach selected pressure regions without materially reducing the calculated line area.

General Tube Model

The acoustic model used throughout this document follows the quarter-wave transmission-line methods developed and documented extensively by Martin J. King. King treats the air within a transmission line as a distributed acoustic system having mass, stiffness, damping, natural frequencies, and associated pressure and volume-velocity mode shapes. His work provides a particularly clear physical description of how the air column behaves inside a quarter-wave loudspeaker and how that behavior relates to driver excitation and terminus output (King, 2002, 2006, 2023).

The simplest reference case is a straight tube with the driver at the closed end and an open terminus. Its first longitudinal resonance occurs approximately when the acoustic length is one quarter wavelength,

$$f_1 \approx \frac{c}{4L}$$

The ideal odd modes are given by

$$f_n \approx \frac{\mathrm{n}c}{4L}, \quad n = 1, 3, 5, \ldots$$

At the closed end, acoustic pressure is maximum and particle velocity is minimum. At the open end, pressure approaches a minimum and particle velocity approaches a maximum. Along the tube, pressure and particle velocity form complementary standing-wave patterns: pressure antinodes coincide with particle-velocity nodes, and pressure nodes coincide with particle-velocity antinodes. In the ideal lossless case, the pressure and particle-velocity fields are 90° apart in time.

Flow/2 begins with this same quarter-wave behavior and adds a continuously tapered area, six unequal-length segments, five folds, and a four-passage S6 terminus. Taper changes the exact resonant frequencies and modifies the ideal sinusoidal mode shapes. King's calculations show that tapered, straight, and expanding transmission lines of equal tuning require different physical lengths and that taper changes the spacing and shape of the higher-order modes. In a tapered line, velocity can also increase strongly toward the open end (King, 2002, 2006, 2023). The straight quarter-wave tube therefore provides the reference model used to describe Flow/2; the following sections examine how its taper, segmentation, folds, internal geometry, and resonators modify that basic behavior.

Blevins (1979, pp. 348–349) gives the acoustic boundary conditions used in the ideal tube model. At a rigid wall, fluid velocity normal to the wall is zero. At an opening into a much larger body of fluid, the dynamic acoustic pressure can be approximated as zero. These conditions establish the familiar quarter-wave pressure and velocity distributions: high pressure and low particle velocity at the closed end, with pressure approaching zero and particle velocity reaching a maximum at the open end. They provide the reference conditions from which the more complex Flow/2 geometry is analyzed.

Figure 1 presents idealized, independently normalized spatial profiles for a lossless line closed at the driver and open at the terminus. Pressure is maximum and particle velocity is zero at the closed end; pressure is zero and particle velocity reaches an antinode in magnitude at the open end. Figure 1 shows the first three odd modes, $n = 1$, $n = 3$, and $n = 5$. With $L = 1.83363$m and $c \approx 343$m/s, the corresponding ideal reference frequencies are approximately 46.77, 140.30, and 233.83 Hz. The 149 Hz and 242 Hz values in King's Figure 19 are frequencies for his specific impedance examples. Flow/2's taper, folds, and internal treatments modify the actual profiles and resonant frequencies. The relationships are derived from King's *Anatomy of a Transmission Line Loudspeaker* (2006, Figure 1, p. 2; Figure 12, p. 28; Figure 19 continued and Figure 20, p. 29).

Figure 1 Idealized Quarter Wave Tube

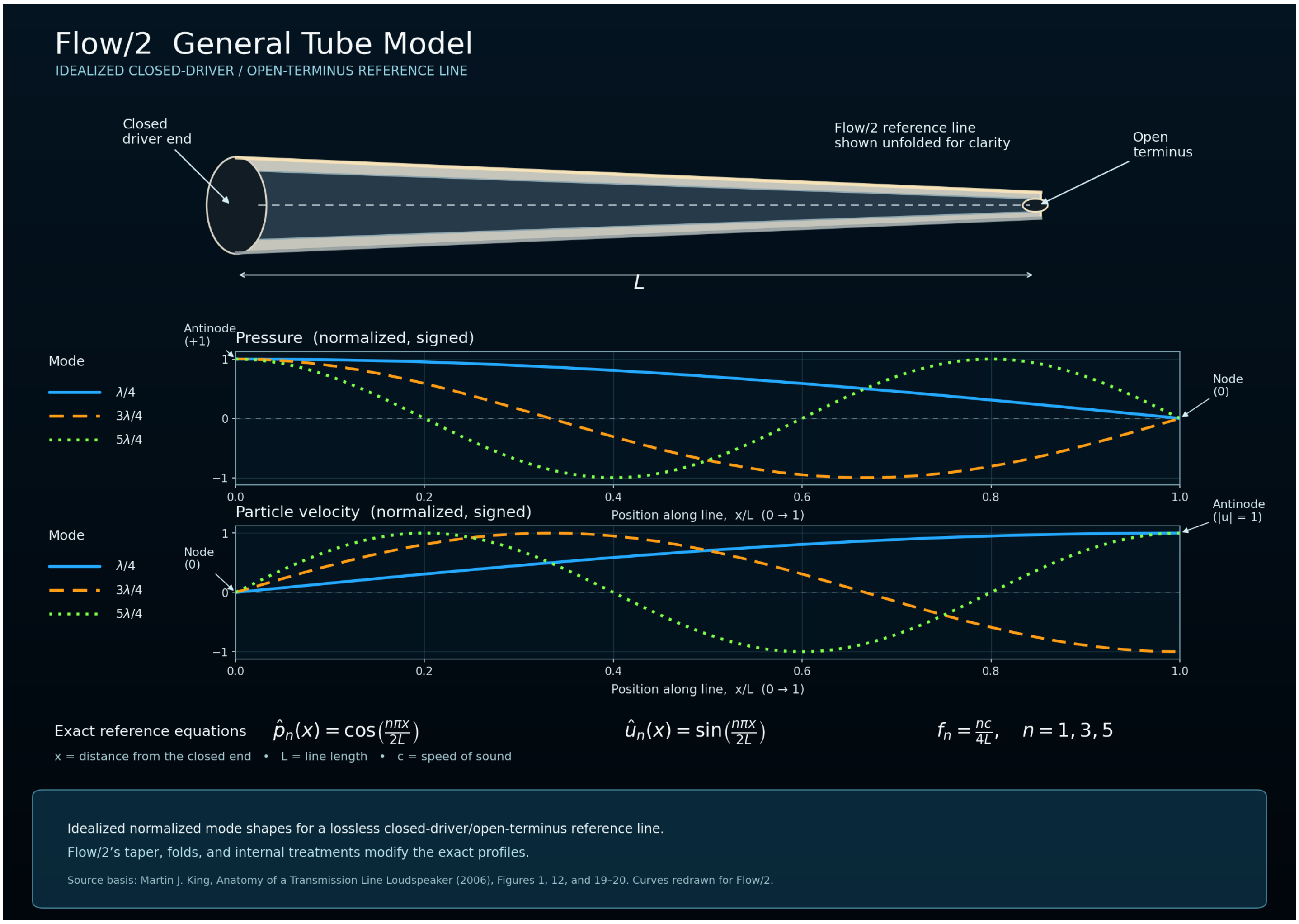

Unequal Length Segments

In Flow/2, the six concentric, coaxial tube segments are unequal in length by design: 259, 269, 286, 304, 325, and 345 mm. Each segment therefore has a different set of axial resonance frequencies and reflection path lengths. This reduces coincidence among the longitudinal standing-wave modes of adjacent segments, spreading their acoustic energy over a wider frequency range and reducing the amplitude of individual resonances.

Unequal segment lengths were also specified in the original folded coaxial transmission-line patent as a means of reducing repeated resonant conditions. The patent describes lower resonance when folded segments have different lengths and gives unequal-length examples including 9, 10, and 11 inches and 8, 10, and 12 inches (Bouvier, 2011). Flow/2 extends this principle across six sections whose lengths increase from 259 to 345 mm, distributing their individual quarter-wave frequencies across a wider frequency range.

The calculations use $f = \frac{c}{(4L)}$, with $c = 343$ m/s. Percentage changes are relative to the preceding segment, as shown in Table 1.

Table 1 Unequal Length Segments.

Segment	Length (mm)	Length change	Ideal quarter-wave frequency (Hz)	Frequency change
S1	259	–	331.1	–
S2	269	+3.86%	318.8	−3.72%
S3	286	+6.32%	299.8	−5.94%
S4	304	+6.29%	282.1	−5.92%
S5	325	+6.91%	263.8	−6.46%
S6	345	+6.15%	248.6	−5.80%

The ideal segment estimates span approximately 331 to 249 Hz. Adjacent frequency estimates differ by approximately 3.7% to 6.5%. Figure 2 plots the relationship between segment length and ideal quarter-wave frequency.

Figure 2 Flow/2 Segment Length and Frequencies.

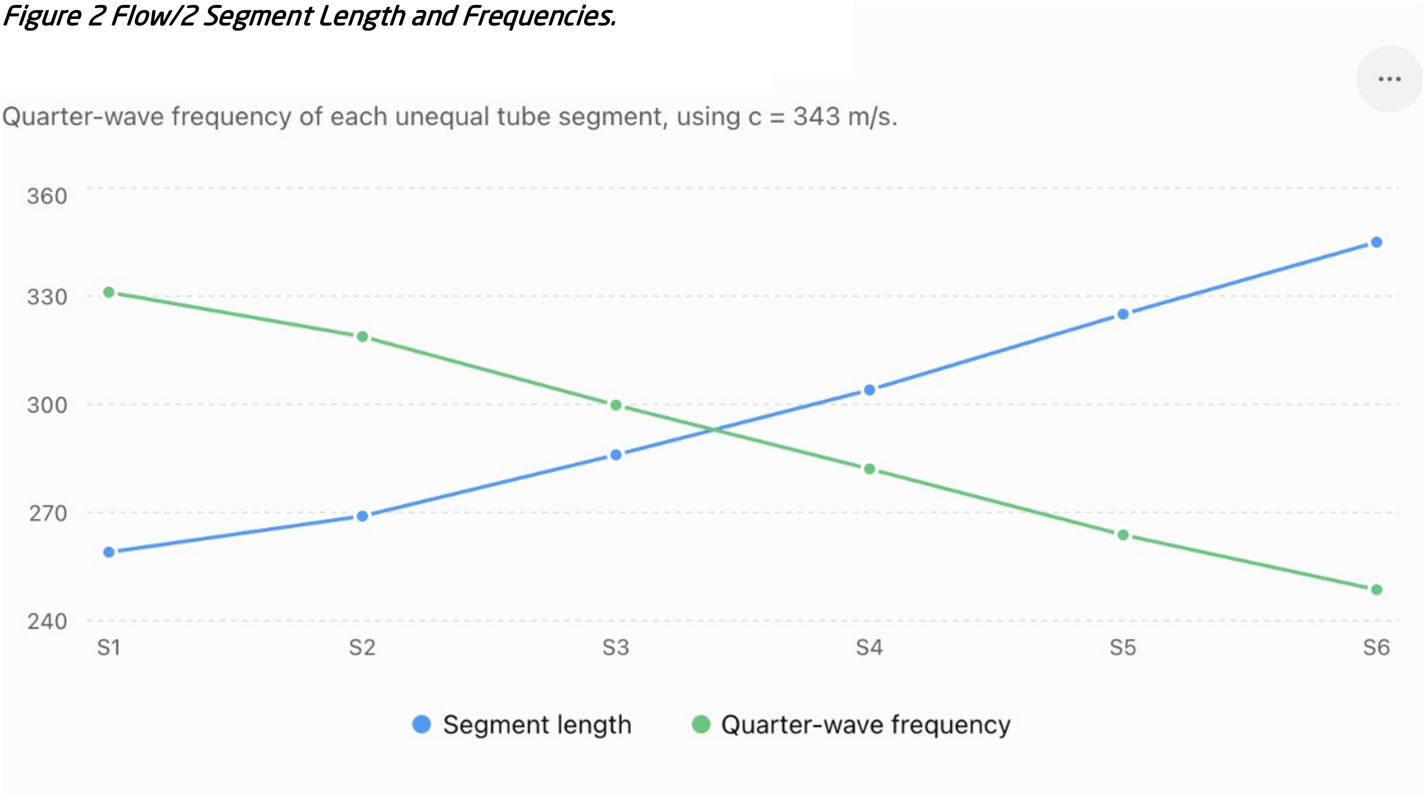

Gyroidic Vanes

The unequal segment lengths begin the process of breaking up repeated behavior from one segment to the next. Flow/2 uses twisted, gyroidic-like vanes in S1 through S5 to interrupt the direct, repeating path through the tube. As each vane twists along its segment, it changes the local section shape and presents a continuously changing set of surfaces to the air-particle motion. The vanes are designed to scatter and redirect higher-frequency acoustic components as they travel through each segment. S6 uses four corner passages and follows a different internal geometry.

The twist sequence alternates direction and varies in magnitude: +90° clockwise in S1, −60° counterclockwise in S2, +55° clockwise in S3, −45° counterclockwise in S4, and +40° clockwise in S5. This sequence is designed to reduce geometric repetition from one segment to the next and lower the likelihood that the same pattern of air-particle motion will recur throughout the line. The vanes add local acoustic resistance and surface area. Their differing orientations distribute those changes across the five segments and reduce geometric periodicity.

The vane structures connect the inner and outer walls of each annular segment, adding support to the printed elements. This geometry is designed to increase local stiffness and reduce wall motion, which may reduce the contribution of structural resonances to the acoustic response. Viewed along the line, the vane arrangement largely interrupts direct line-of-sight toward the successive folds, creating a more tortuous path for the air motion with the intended effect of reducing direct axial transmission.

Blevins (1979, pp. 345–349) provides analytical mode shapes for annular acoustic volumes. The solutions identify mode families by axial nodes, nodal diameters, and nodal circles, establishing that an annular passage can support axial, circumferential, and radial pressure patterns. Flow/2's S1 through S5 passages have this annular character, with taper, folds, and changing boundary geometry altering the ideal mode shapes. The twisted vanes continuously change the section geometry and surface orientation along each segment, reducing the repeated annular geometry available to support organized higher-order modes.

Together, these features are designed to reduce the strength and modal Q of longitudinal standing-wave modes, lowering the amplitude and sharpness of tube-generated peaks and dips. Preserving the line's low-frequency quarter-wave loading remains a design requirement.

The acoustic effects described here are design objectives and predictions. Measurements of impedance, near-field driver and terminus response, phase, and decay will establish the result after the Flow/2 enclosure has been printed.

Figure 3 shows the vane geometry for S1 through S5, the combined arrangement, and top-down and bottom-up views of the tube segment. Vanes in each segment are twisted to interrupt direct axial transmission and disturb repeated reflection paths. The twist also reduces direct line of sight from the bezel toward the base.

Figure 3 Gyroidic Vanes.

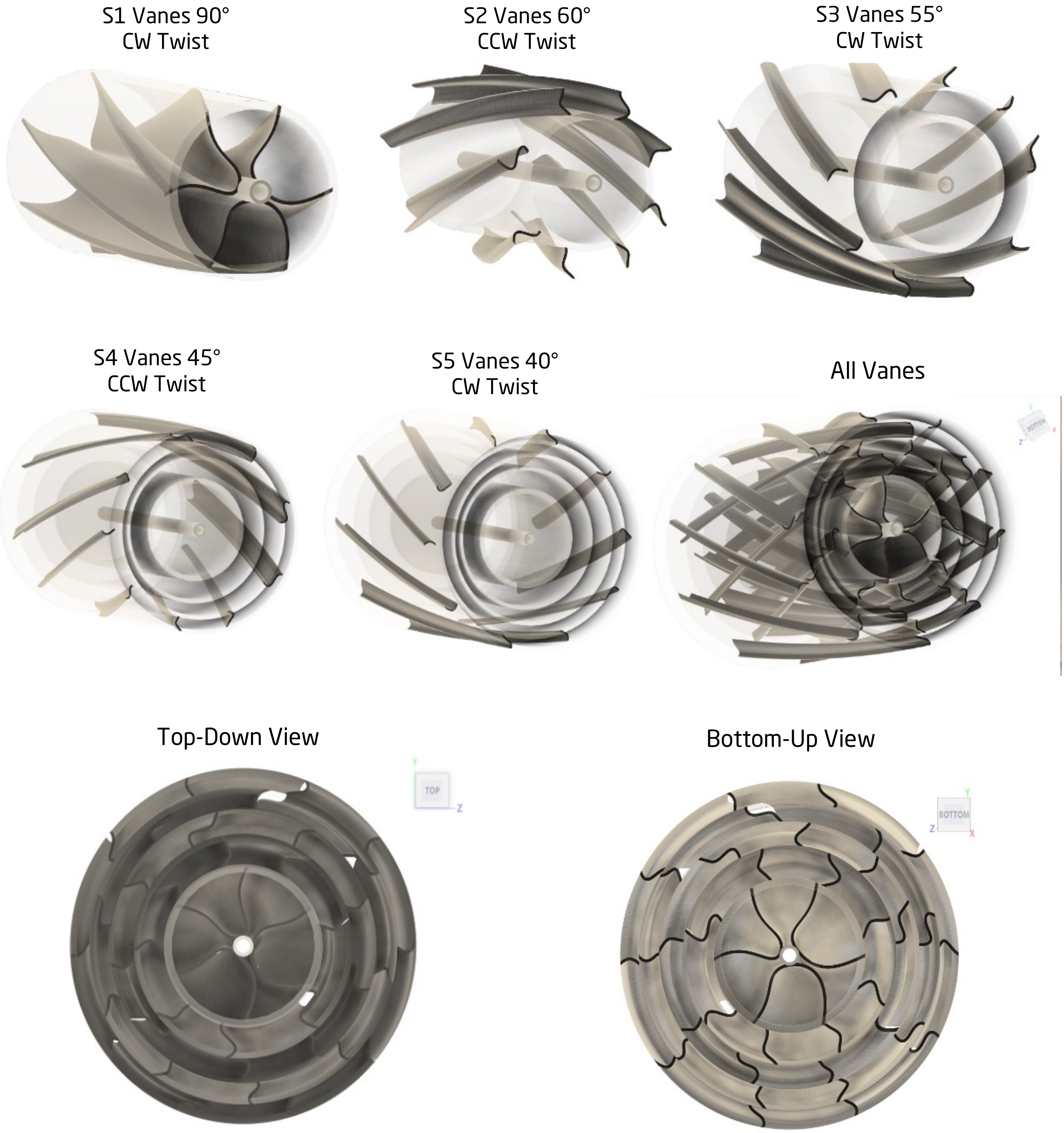

Figure 4 shows right-side, front-side, and diagonal sectional views of Flow/2. The sections reveal the vane structures within the tubes and several Helmholtz resonators in the bezel and base. The throat of the 149 Hz bezel resonator is visible in the right-side section, and its chamber is visible in the front-side section. The diagonal base section shows the throat and chamber of the 432 Hz resonator and the throats and chambers of two of the four 239 Hz resonators.

Figure 4 Section Views of Vanes.

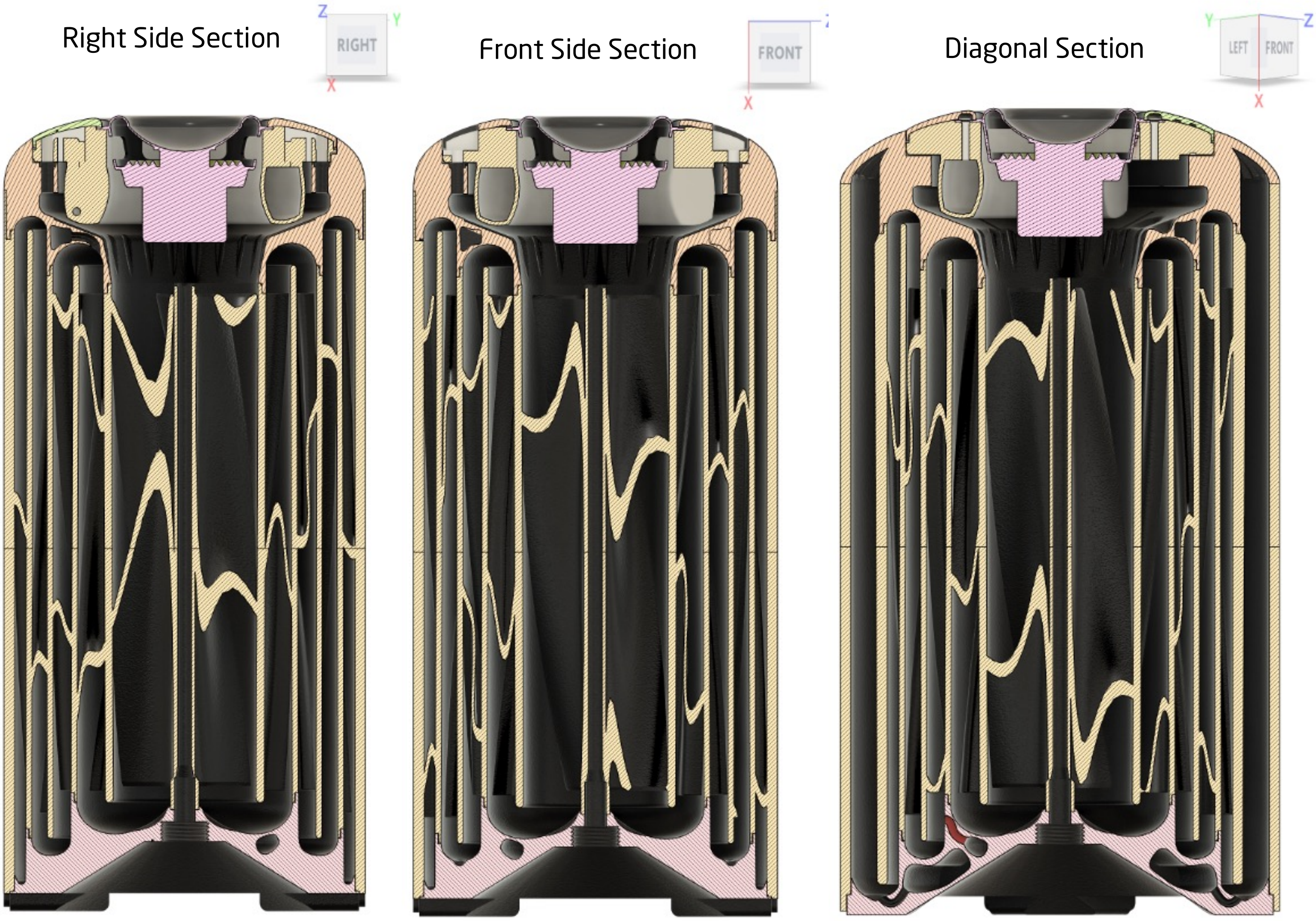

Dimples, Pimples, and Clefts

The gyroidic vanes disturb the acoustic path within each segment. The folds introduced another problem: each fold changes the direction of the acoustic path and creates a place where transmitted and reflected waves meet. Broad, smooth surfaces can return similar reflections along similar paths, allowing pressure patterns to build at particular frequencies.

I added dimples, pimples, and clefts at selected necks, folds, and transitions. In this design, dimples are shallow concave depressions, pimples are rounded convex protrusions, and clefts are narrow grooves or interruptions in otherwise continuous surfaces. Each feature changes the local boundary shape, causing reflected energy to follow different paths and return with different phases and directions. Together, these features are intended to disturb repeated pressure patterns and reduce coherent addition from fold to fold.

These features act locally. They modify reflections at folds and transitions, and the global quarter-wave modes remain part of the line's operation. The design objective is to lower the modal Q of higher-order tube modes and reduce the amplitude and sharpness of tube-generated peaks and dips. The line's low-frequency quarter-wave loading remains a design requirement.

Figure 5 shows the locations of the dimples, pimples, and clefts within the Flow/2 enclosure. The acoustic effects described here are design objectives and predictions. Measurements of impedance, near-field driver and terminus response, phase, and decay will establish their effect in the printed enclosure.

Figure 5 Dimples, Pimples, and Clefts.

Antinode Helmholtz Resonators

The geometric treatments are designed to distribute reflected energy through the line. Calculations identified four frequency regions associated with higher-order longitudinal modes, so Flow/2 adds seven tuned Helmholtz resonators to address them.

A Helmholtz resonator is an enclosed air cavity connected to an acoustic passage through a narrow neck. The air in the neck behaves as an acoustic mass, and the compressibility of the air in the cavity provides a spring. Together, they form a tuned side branch that responds strongly over a narrow frequency range. When the neck opens near a pressure antinode of a targeted tube mode, acoustic energy is diverted into the resonator. Losses in the neck, cavity walls, and surrounding structure dissipate part of that energy, reducing the mode's pressure peak and Q (Lloyd, 1968; Selamet & Ji, 2000).

Flow/2 uses seven resonators at approximately 149, 239, 335, and 432 Hz. The 239 Hz treatment uses four identical resonators, one for each S6 corner passage. The resonators supplement the unequal segment lengths, twisted vanes, and irregular fold geometry. Their frequency-selective loading is intended to reduce selected higher-order modes. The line's useful low-frequency quarter-wave loading remains a design requirement.

Each neck opening is positioned at or near a calculated pressure antinode for its target mode. The chamber can occupy available volume in the bezel or base. The neck dimensions, end correction, and effective length remain part of the tuning. A neck may open through a tube wall, into a fold, or project slightly into the acoustic passage. Printing tolerances, losses, neck end correction, and the actual folded geometry can shift the final tuning, so measurements of the completed loudspeaker will establish the final frequencies.

Table 2 Helmholtz Resonator Locations.

Target frequency	**Tube mode**	**Neck-opening region**	**Chamber location**	**Function**
~149 Hz	Odd-order mode n = 3	Driver/bezel end of line	Unused volume within the bezel	Reduces the strongest low-order unwanted line mode
~239 Hz, four units	Odd-order mode n = 5	S5-to-S6 transition, with necks extending into S6	Four chambers embedded in base	Reduces the next higher longitudinal mode
~335 Hz	Odd-order mode n = 7	S2-to-S3 fold	Embedded in bezel	Reduces higher-order line energy
~432 Hz	Odd-order mode n = 9	S3-to-S4 fold	Embedded in base	Reduces upper line-mode output and stored energy

The resonators operate together with the unequal segment lengths, twisted vanes, and irregular fold surfaces. The geometric features disturb standing-wave formation throughout the line. The Helmholtz resonators add frequency-selective loading and dissipate part of the energy associated with the remaining dominant modes.

Figure 6 shows the seven resonators embedded in Flow/2: the 149 Hz and 335 Hz resonators in the bezel, four 239 Hz resonators in the base, and the 432 Hz resonator in the base.

Figure 6 Helmholtz Resonators.

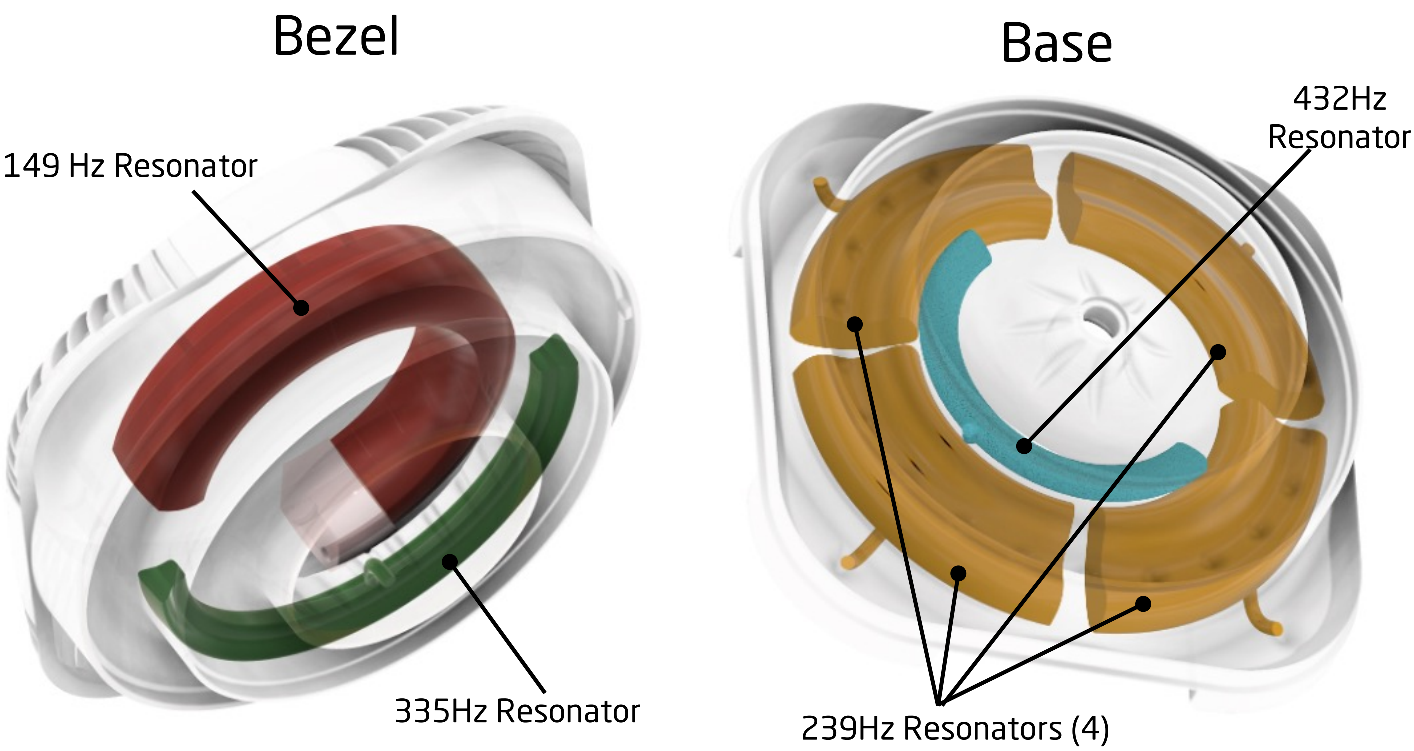

The 149 Hz resonator is located in the bezel near the driver, where the line presents a pressure antinode for its low-order longitudinal modes.

Using the 1,788 mm straight-segment coordinate, excluding fold lengths, the 239 Hz mode has a calculated pressure antinode at approximately 1430 mm, 13 mm before the S5-S6 fold in the base at 1443 mm. The resonators are positioned at the S5-S6 transition, with their necks extending approximately 5 to 10 mm into S6. Because S6 is divided into four separate corner ducts, the 239 Hz treatment uses four identical single-neck resonators, one connected to each duct. Equal resonator geometry gives the four S6 paths equal acoustic loading. Separate chambers prevent a common resonator cavity from coupling those paths through the resonator system.

The four 239 Hz resonators use separate cavities as well as separate throats. A single cavity connected to all four S6 passages would form a multi-neck Helmholtz resonator whose neck air masses interact through the common chamber. Papadakis and Stavroulakis (2023) show that multi-neck Helmholtz resonators introduce interaction among the individual neck air masses through the common cavity, with increasing uncertainty in effective neck length as neck count increases. Flow/2 therefore uses four independent single-neck resonators for the 239 Hz treatment, one for each S6 passage. This keeps the four acoustic paths separately loaded, preserves symmetry among them, and simplifies calculation and tuning.

The 335 Hz mode has a calculated pressure antinode at approximately 511 mm, 17 mm before the S2-S3 fold in the bezel at 528 mm. This establishes the location of the 335 Hz resonator.

The 432 Hz mode has a calculated pressure antinode at approximately 795 mm, 19 mm before the S3-S4 fold in the base at 814 mm. This establishes the location of the 432 Hz resonator.

These frequencies and positions come from the calculated upper longitudinal modes of the modeled Flow/2 tube. The selected antinode locations provide strong coupling to the target modes and divert acoustic energy into the side branches. Resonator losses are expected to dissipate part of that energy, reducing the corresponding pressure peaks and modal Q. Measurements of impedance, near-field driver and terminus response, phase, and decay will establish how closely the printed enclosure meets these design objectives.

Helmholtz Resonator Rationale

The use of side-branch Helmholtz resonators in Flow/2 is supported by established duct-acoustics research. A Helmholtz resonator presents a frequency-dependent acoustic impedance to the main passage. Near its tuned frequency, the air mass in the neck oscillates against the compliance of the enclosed air volume, producing a strong local response that can reduce acoustic transmission at that frequency. Pipe-mounted Helmholtz resonators have been analyzed and tested for this purpose, including the effects of neck geometry, cavity geometry, connection geometry, and neck end correction (Selamet & Ji, 2000).

This narrow-band response is particularly useful in Flow/2 because the frequencies to be treated are known higher-order resonances of the tapered quarter-wave line. Separate resonators can therefore be tuned near approximately 149, 239, 335, and 432 Hz while leaving the wanted low-frequency quarter-wave response substantially unaffected. Side-branch resonators can be designed for specified attenuation frequencies and can use asymmetric cavities, multiple necks, and other geometries suited to restricted available spaces (Li et al., 2026).

Placement of the neck opening is also important. A Helmholtz resonator couples most strongly to a standing-wave mode where acoustic pressure is high. Experimental work by Lloyd (1968) examined resonator placement at pressure nodes and antinodes and demonstrated the importance of positioning the resonator at a pressure maximum for effective damping. In Flow/2, the neck openings are therefore located at, or close to, calculated pressure maxima of the targeted line modes. The sealed chambers themselves may be located elsewhere in the bezel or base and connected to those positions by their necks (Lloyd, 1968).

The approximate Helmholtz tuning frequency is

$$f_H = \frac{c}{2\pi}\sqrt{\frac{A_N}{V_C L_{\mathrm{eff}}}}$$

where A_N is the neck cross-sectional area, V_C is the enclosed chamber volume, and L_{eff} is the effective acoustic length of the neck. The effective length includes the physical neck plus acoustic end corrections caused by the motion of air immediately outside its openings. Neck location, cavity geometry, and dimensional transitions can therefore shift the actual resonance from the value predicted by the elementary equation (Selamet & Ji, 2000). For this reason, the calculated Flow/2 resonator dimensions establish the initial tuning, with final frequencies verified by measurement.

Blevins (1979, pp. 353–360) describes the Helmholtz resonator as the acoustic equivalent of a spring-mass oscillator. The compressibility of the cavity air provides the spring, with an equivalent stiffness

$$k = \frac{\rho c^2 A^2}{V},$$

and the air moving in the neck provides the mass,

$$M = \rho A L.$$

Substitution into the spring-mass natural-frequency equation gives the familiar Helmholtz relationship

$$f_H = \frac{c}{2\pi}\sqrt{\frac{A}{VL}}.$$

This model assumes a nearly uniform cavity pressure and treats the neck air as a concentrated acoustic mass. Blevins also notes that the elementary formula neglects the inertia of fluid within the cavity and the motion of fluid immediately outside the neck. These effects become more important as the neck becomes short relative to its diameter or as the neck dimensions approach those of the cavity. Effective neck length and end correction are therefore included in the Flow/2 resonator calculations.

In a small-signal model, the Helmholtz branch impedance can be written

$$Z_H = R + j\left(\omega M - \frac{1}{\omega C}\right)$$

where R represents acoustic resistance, M the effective neck air mass including end correction, and C the cavity compliance (Guimarães & Ribeiro, 2018). Below resonance, the compliance term dominates. At resonance, the mass and compliance reactances cancel. Above resonance, the neck-mass term dominates. The resonator therefore presents a strongly frequency-dependent acoustic load to the tube, allowing selected modes to be treated with little effect at frequencies far from the resonator tuning.

The Helmholtz resonators work with the other mode-control features of Flow/2. Unequal segment lengths reduce repeated axial conditions, the twisted vanes disturb transverse and circumferential standing-wave patterns, and the dimples, pimples, and clefts modify reflection conditions at the folds. The Helmholtz resonators then provide targeted treatment of the remaining low-order longitudinal line resonances. Their purpose is to reduce the amplitude and Q of those unwanted modes while retaining the useful quarter-wave loading of the line.

The Folds

In Flow/2, the six segments are connected by folds. Folds are designated F1 through F5, and segments are designated S1 through S6. S1 through S5 are annular ring segments. S6 consists of four corner passages whose combined clear area is designed to equal the area of one segment. S6 forms the final segment and feeds the terminus. Figure 7 illustrates the segment and fold relationship.

Figure 7 Diagonal Section View of Folds.

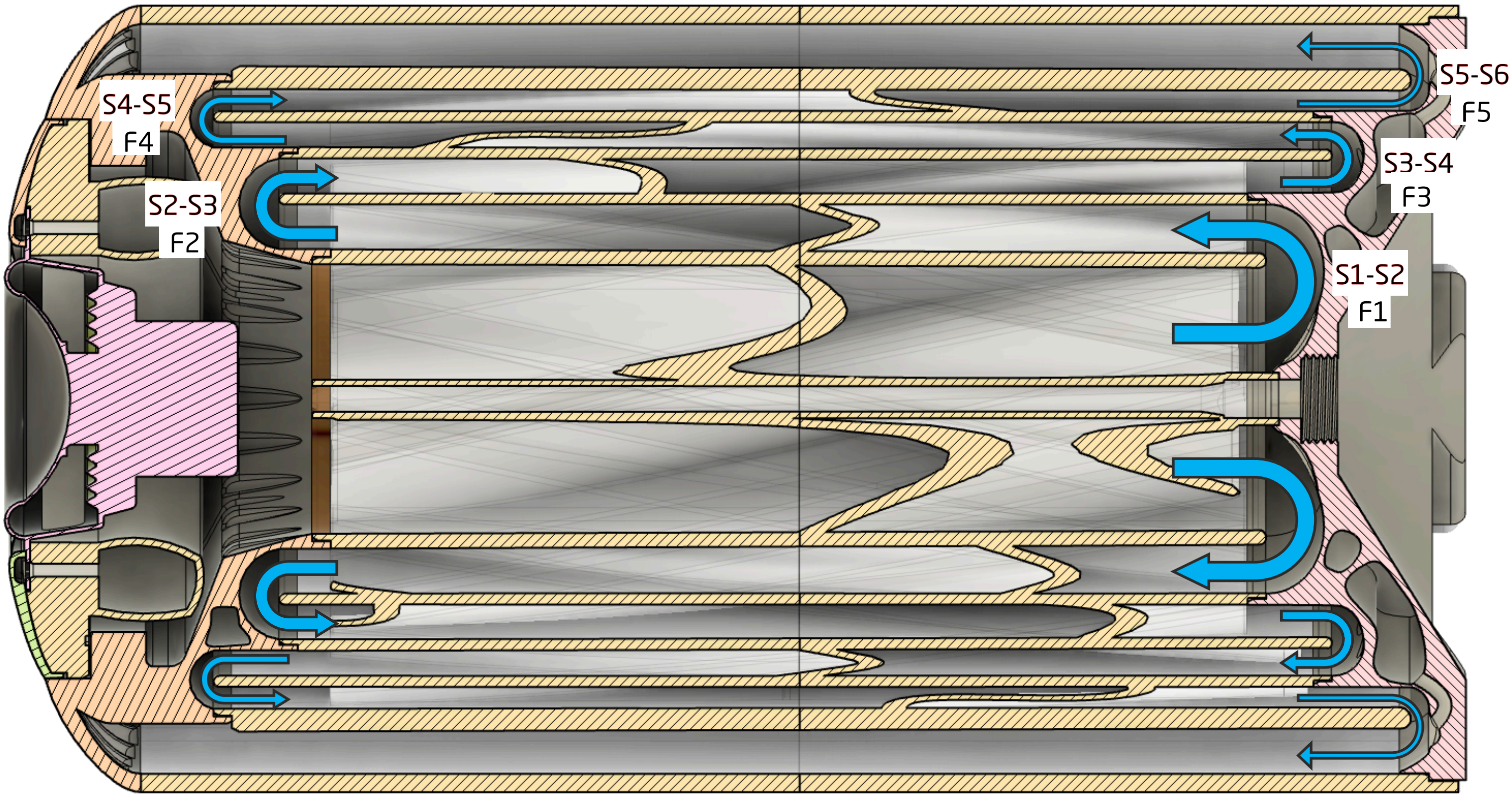

The acoustic path follows the centerline through the segments and folds and measures 1,833.63 mm in the current design. Each fold changes flow direction and creates a local region with its own cross-sectional area, curvature, boundary-layer behavior, and acoustic impedance (Augspurger, 2000; Rienstra, 2005).

Flow/2 uses four folds between ring segments S1 through S5. Their centerline lengths are approximately 15.5, 11.1, 8.8, and 6.5 mm. At the S5-to-S6 transition, the line divides into four corner passages. Each passage has a curvilinear quadrilateral cross-section bounded by an inner circular arc, an outer rounded-corner fillet, and two adjacent enclosure walls. The transition zone separates and directs the wavefront from S5 into four channels and maintains the required clear area for flow in either direction. The 5.325 mm S5-to-S6 vertical dimension describes the transition and clearance at that junction. Figure 8 illustrates this transition.

Figure 8 S5-S6 Transition Area.

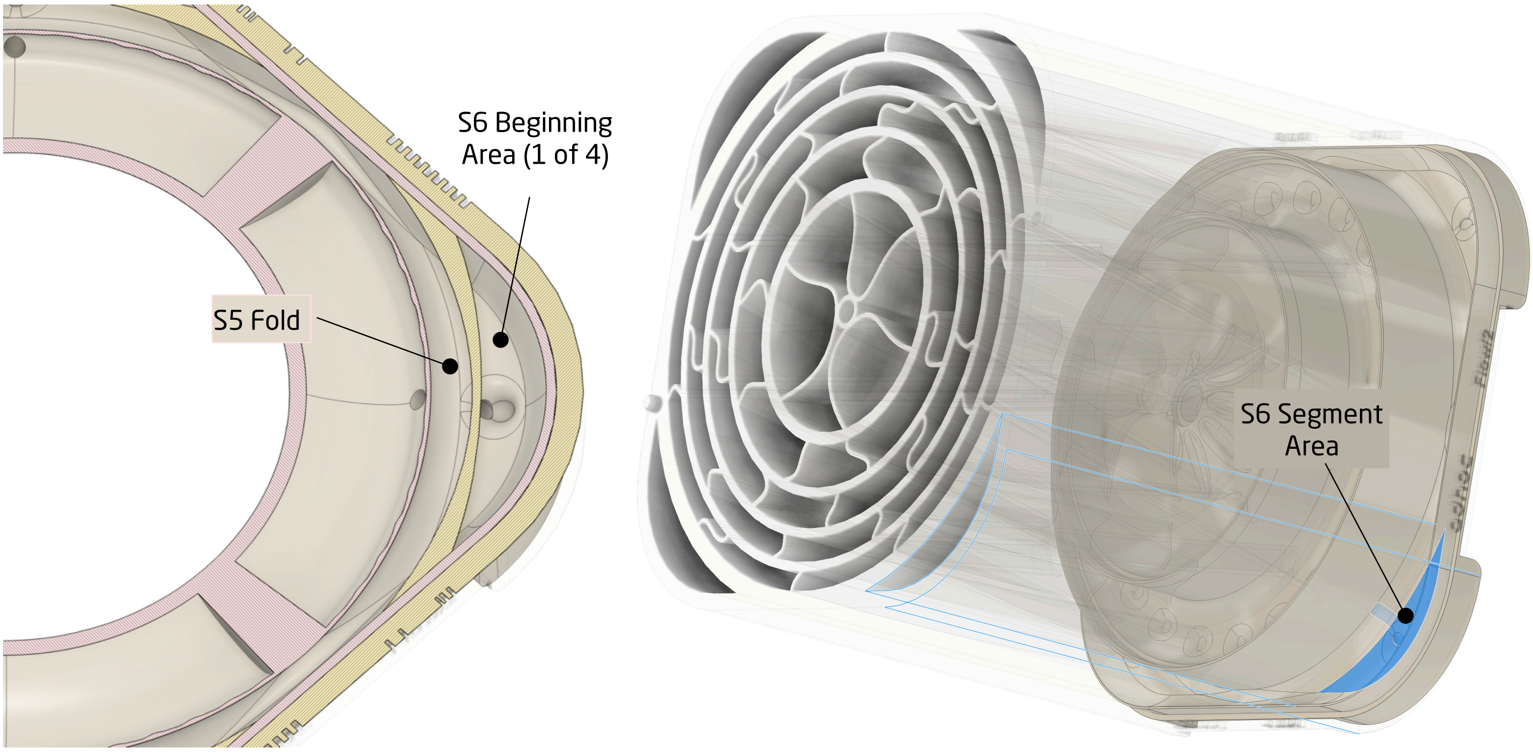

Flow/2 is based on the Dayton Audio ND91-8 driver, which has an effective piston area (Sd) of 3,040 mm² (Dayton Audio, n.d.). The line tapers from a net clear area of 3,800 mm² at the S1 beginning to 2,280 mm² at the S6 terminus.

At the S5-to-S6 interface, the target clear-air area is 2,582 mm² on both sides. S5 includes a 223 mm² vane, so its gross end profile is 2,805 mm²; its clear-air area is 2,582 mm². The S5 gross profile includes the vane area and serves as the geometric envelope. S6 corner passages contain no vanes, so their area measurements are clear-air areas.

At a fold, the incident wave divides into transmitted and reflected components. A curved, tangent transition spreads the impedance change over distance, while an abrupt step produces a stronger local reflection. Reflection can maintain a standing-wave pattern; viscous and thermal wall losses remove part of the acoustic energy. A fold does not by itself establish a lower modal Q. A one-dimensional section model can provide a starting estimate, while a full three-dimensional model or measurement is required for the detailed bend response. Jackson (2005) used finite-difference time-domain analysis to study the discontinuity of a folded acoustic line, and Rienstra (2005) treats slowly varying and bent ducts within the Webster framework.

Tube Characteristics

For the established Flow/2 acoustic path:

$$\phi = \frac{2\pi f L}{c}$$

where ϕ is accumulated propagation phase, f is frequency, L is the centerline path length, and c is the speed of sound.

The total line length, which is the sum of the segment lengths, folds and transitions, is 1,833.63 mm. At c = 343 m/s, the ideal quarter-wave propagation-delay frequency is:

$$f_{90^\circ} = \frac{c}{4L} = \frac{343}{4(1.83363)} = \boxed{46.77\ \text{Hz}}$$

Thus, the ideal quarter-wave propagation-delay frequency is approximately 46.77 Hz. The one-way line delay is approximately 5.35 ms, and the period at 46.77 Hz is 21.38 ms. A peak inward velocity reaches the terminus one quarter period later, when the diaphragm is at displacement reversal. The calculated tapered-line resonance, approximately 41.98 Hz, is a separate model result. At 41.98 Hz, the 1,833.63 mm path corresponds to approximately 80.8° of propagation phase.

The colors in Figure 9 show normalized pressure magnitude, $|\ p\ |$, at 46.63 Hz. Red indicates high pressure and blue indicates low pressure. The modeled first mode has one positive pressure lobe. Standing-wave pressure phase is continuous through S1–S6 and is approximately 0°within this positive lobe.

The open terminus approaches a pressure node, and particle velocity approaches a maximum. In the lossless standing-wave reference, pressure and particle velocity are 90° apart in time.

The reduced-order equation should be written as:

$$\frac{d}{ds}\left[A(s)\frac{dp}{ds}\right] + k^2 A(s)p = 0$$

The reduced-order equation uses s for distance along the tube centerline, A(s) for local clear line area, p(s) for acoustic pressure at that position, and k = 2πf/c for acoustic wavenumber, where f is frequency and c is the speed of sound. It is a one-dimensional form of Webster's horn equation for a slowly varying tube (Rienstra, 2005; Stinson, 1991).

Figure 9 Quarter-Wave Pressure Map.

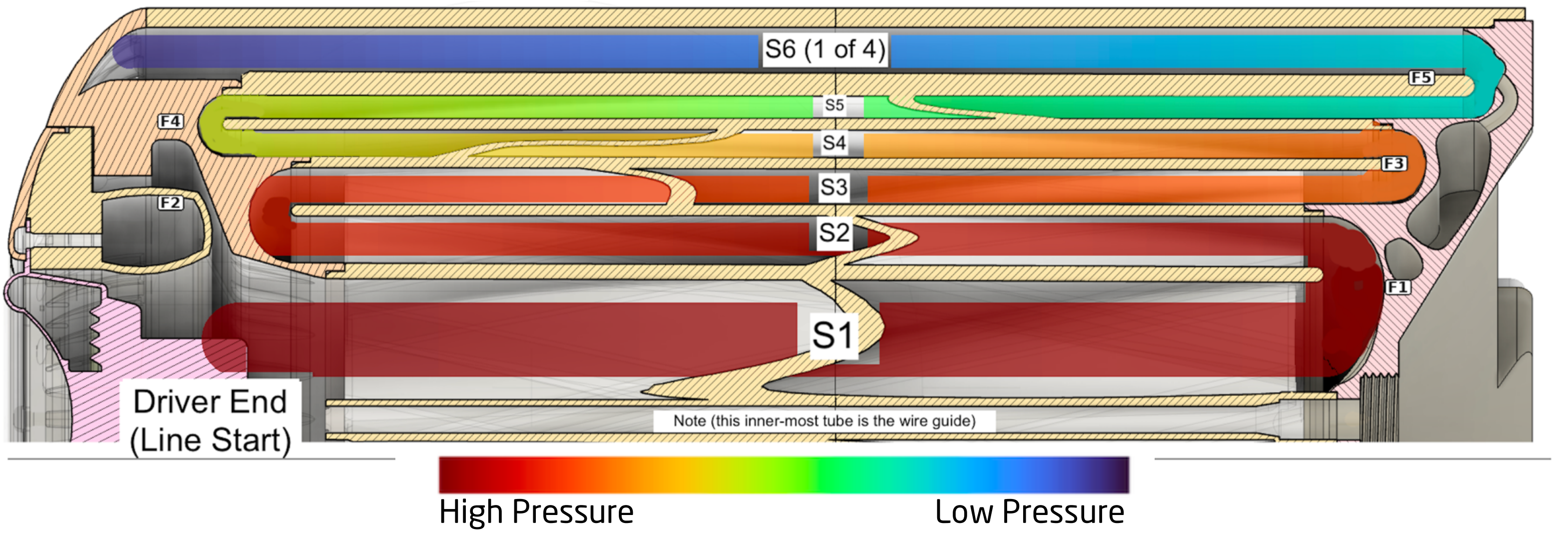

At a smooth fold, acoustic pressure remains continuous through the connected passage, and the particle-velocity vector turns with the passage. Maintaining the net clear area reduces an abrupt characteristic-impedance change. At the 46.63 Hz model frequency used for Figure 9, the period is 21.45 ms, the one-way line delay is 5.35 ms, and the accumulated propagation phase is approximately 89.7°. A quarter-period is 5.36 ms. The tapered-line open-end mode is calculated at approximately 41.98 Hz. At 46.63 Hz, the modeled exit pressure is 0.183 times the driver-end pressure.

The same continuous-passage condition applies at each fold. The small modeled pressure changes across the short fold lengths are shown in Table 3. The pressure values are normalized to the driver-end pressure.

Table 3 Fold Pressure Changes.

Fold	Before	After	Δp
F1	0.975	0.972	-0.003
F2	0.890	0.885	-0.005
F3	0.736	0.731	-0.005
F4	0.508	0.502	-0.006
F5	0.201	0.192	-0.009

These changes arise from propagation over each fold length. At the 46.63 Hz model frequency, the inward-peak pulse arrives after approximately 5.35 ms, essentially one quarter-period, or 5.36 ms, later. The diaphragm is at reversal; outward motion begins immediately afterward.

For a centerline path length of 1,833.63 mm, the ideal quarter-wave frequency based on propagation delay is 46.77 Hz.

At 46.77 Hz, the 1,833.63 mm path has a one-way delay of approximately 5.35 ms, corresponding to a propagation phase of approximately 90.0°. The driver-end and line-end traveling-wave components therefore combine in quadrature. Their resultant amplitude is the root-sum-square of the two amplitudes. Maximum in-phase reinforcement requires zero total relative phase at the listening position, including driver and port-radiation phases.

At 46.77 Hz, all seven Helmholtz resonators remain below their target frequencies. The 149 Hz bezel resonator is closest to tuning and is expected to show the largest response. The four 239 Hz resonators at the S5-to-S6 transition should have small, mostly reactive throat flow.

The 335 Hz resonator at the S2–S3 fold sees a relatively strong local pressure drive, though it remains far below resonance.

The 432 Hz resonator near the S3–S4 fold is the most detuned and should have the smallest response.

In every chamber, pressure should be nearly uniform. Pressure gradients concentrate in the short throats, reverse direction every half-cycle, and remain modest at this frequency. Exact local values require the resonator impedances and a three-dimensional pressure-acoustics model.

Air Velocity Through the Folds: Chuffing Risk

The airflow analysis was extended to the Dayton Audio ND91-8's published linear excursion limit of ±5.1 mm (Dayton Audio, n.d.). The resulting values are used to assess whether the folds, the S5-to-S6 transition, or the exit system could generate appreciable turbulence or audible "chuffing."

For sinusoidal diaphragm motion, peak driver volume velocity is

$$U_{pk} = S_d\ 2\pi f X$$

where

$$S_d = 3040\ \text{mm}^2$$

and

$$X = 5.1\ \text{mm}.$$

At 30 Hz, the resulting peak driver volume velocity is approximately 2.92 L/s. At 60 Hz it is approximately 5.85 L/s. Applying these values directly to the calculated net tube areas gives the area-average velocities in Table 4.

Table 4 Air Velocity through Folds @Xmax.

Location	Net area (mm²)	30 Hz peak velocity (m/s)	60 Hz peak velocity (m/s)
S1 beginning	3800	0.77	1.54
Fold 1	3581	0.82	1.63
Fold 2	3353	0.87	1.74
Fold 3	3110	0.94	1.88
Fold 4	2852	1.03	2.05
Fold 5	2582	1.13	2.27
S6 end	2280	1.28	2.56

The velocity progression follows the tube taper. Each fold maintains approximately the same net area as the end of the preceding segment and the beginning of the following segment. Area-average velocity therefore remains nearly constant while the air traverses the fold. The fold changes direction without introducing contraction. Broad radii and rounded inner and outer surfaces reduce local acceleration and the tendency toward flow separation during the turn.

Flow/2 is a quarter-wave system, so local volume velocity varies considerably with position and frequency. Near the first longitudinal mode, the air motion near the later segments of the line becomes substantially greater than the volume velocity behind the driver. The line's volume-velocity maximum occurs at approximately 42 Hz.

At the Dayton Audio ND91-8's rated ±5.1 mm excursion, the calculated linear-model velocities in this region are shown in Table 5:

Table 5 End Segment Velocities @Xmax.

Frequency	F5 peak velocity	S6-end peak velocity	Exit-grille peak velocity
40 Hz	16.5 m/s	19.4 m/s	3.94 m/s
41 Hz	19.7	23.2	4.72

Frequency	F5 peak velocity	S6-end peak velocity	Exit-grille peak velocity
42 Hz	18.7	22.0	4.48
43 Hz	15.1	17.8	3.62
45 Hz	9.70	11.5	2.34
47 Hz	7.03	8.38	1.70
50 Hz	5.05	6.06	1.23

These resonance-region values are upper estimates from a linear model. At the largest predicted velocities, aerodynamic resistance, viscous loss, flow separation, vortex formation, and compression progressively reduce the actual acoustic gain. Rapoport and Devantier (2004) report the onset of port-flow instabilities in their tested conditions at approximately 5–10 m/s and associate increasing air velocity with turbulence, distortion, noise, and compression. Salvatti et al. (1998) likewise identify high-velocity turbulent airflow as the source of broadband “chuffing” and show that aerodynamic shaping and rounded terminations improve compression, efficiency, maximum output, and distortion performance.

The highest calculated velocities occur at F5 and S6 near the first quarter-wave mode. Flow/2 addresses this region geometrically. The S5-to-S6 transition preserves the required aggregate area as the annular S5 passage divides into four S6 passages. Its increased depth compensates for area displaced by the square enclosure geometry, and the recessed dimples, large fillets, and rounded surfaces increase local passage volume and reduce abrupt changes in the flow path. The four S6 passages then continue toward the end of the line with equal nominal areas.

Later work provides additional support for the importance of fold and transition geometry. Bezzola et al. (2019) identify flow separation and vortex shedding as principal sources of port noise and show that appropriately shaped flares permit higher operating velocities before unwanted blowing noise develops. Their review also reports that bends and corners can degrade performance and that smooth geometry reduces this effect. Bezzola et al. (2020) subsequently measured straight, bent, and flared ports and found that poor flaring and bends can increase acoustic resistance, compression, and port noise as drive level rises. Their measurements further showed that gentle bends produced better results than sharp bends, and that straight and optimally flared ports exhibited the least compression and port noise.

Each corner grille provides approximately 2,803 mm² of open area, about 4.9 times the corresponding S6 terminus area. Consequently, even during the calculated 41 to 42 Hz maximum, average grille velocity remains below 5 m/s. The permanent grille uses rounded edges throughout, and its stepped entry region distributes the final area increase over several smaller changes. The grille therefore remains well below the velocity reached inside S6 and is unlikely to become the controlling source of airflow noise.

For ordinary program material, continuous full-Xmax excitation at one low frequency is an unusually severe operating condition. At the rated ±5.1 mm linear excursion, the calculations show substantial airflow margin through F1 through F4. F5 and S6 carry the greatest local velocity and consequently define the region most likely to approach nonlinear airflow behavior near the first quarter-wave mode. The next question is how the system behaves at the nonlinear excursion levels the Dayton Audio ND91-8 can actually reach.

Airflow at Nonlinear Xmax Extremes

The Dayton Audio ND91-8 has also been observed to move considerably beyond its rated ±5.1 mm linear Xmax. To examine the tube geometry under a much more severe condition, the airflow calculations were repeated at ±10 mm excursion. This is well outside the driver's specified linear operating range and serves as a stress test of the acoustic passage.

At ±10 mm, peak driver volume velocity is approximately twice the rated linear Xmax value. The corresponding local velocities therefore rise by approximately the same factor so long as the system is treated as linear.

At 40 Hz, the model predicts approximately 32 m/s through F5 and 38 m/s at the S6 end (the end of the line). The large exit area reduces average grille velocity to approximately 7.7 m/s. At 47 Hz, the corresponding values are approximately 13.8 m/s at F5, 16.4 m/s at the S6 terminus, and 3.3 m/s through the grille.

These ±10 mm calculations extend the model into conditions where the system becomes nonlinear. Aerodynamic resistance rises, separation and vortex formation become more likely, and acoustic compression reduces the attainable quarter-wave gain.

The calculated 32 to 38 m/s values are linear-model predictions that show the very high airflow demand at these excursion levels. At these extreme excursions, audible flow noise becomes plausible near F5 and the S6 terminus.

The geometry provides additional flow margin: the folds contain no discrete area restriction, the S5-to-S6 division preserves aggregate area, the major transitions are rounded, and the exit grille presents a much larger flow area than the S6 terminus. The limiting condition at extreme excursion is the high local air velocity generated by the resonant line.

Impact of the Folds

The folds introduce two principal effects into the Flow/2 line. Their short, constant-area sections, each with a different length, interrupt the continuous taper slope for a few millimeters, and their curvature redirects the moving air. The calculated departures from the ideal taper are small, and the matched areas at each segment-to-fold interface avoid sudden velocity changes. Turning loss and viscous loss remain, with their influence increasing toward the later folds as tube area decreases and air velocity rises.

F5 is the most demanding fold because it carries the highest fold velocity and divides the annular S5 flow into four S6 passages. Its compensated depth, dimples, fillets, rounded surfaces, and matched aggregate area address that condition. F1 through F4 operate at substantially lower velocities and present little indication of becoming sources of audible flow noise at rated driver excursion.

Taken together, the calculations identify no discrete area restriction in the Flow/2 folds. They still predict approximately 18–23 m/s in F5 and S6 near 41–42 Hz, so flow separation, compression, and audible airflow noise remain empirical questions at rated Xmax. The rounded geometry is intended to reduce that risk. The matched fold areas avoid discrete velocity increases, and the broad radii and rounded surfaces address the bend-related losses reported in the literature (Bezzola et al., 2020; Rapoport & Devantier, 2004). Near 41 to 42 Hz, F5 and S6 experience the greatest resonantly increased air velocity, placing these regions closest to the flow-separation conditions described experimentally in loudspeaker-port studies. At the extreme ±10 mm stress condition, audible airflow effects become plausible near F5 and the S6 terminus. The model identifies no fold or grille area acting as a discrete choke point; the limiting condition is the magnitude of the resonantly increased air velocity.

The Exit Port and Grille

S6 is the final tapered segment. Its four corner passages carry the acoustic wave to the termination region, where it couples to the radiation impedance at the grille openings (Levine & Schwinger, 1948).

The S6 terminus opens into an expanding exit chamber formed by the bezel geometry, as illustrated in Figure 10. From the 570 mm² end area of each S6 corner passage, the available open area increases progressively toward the external grille. The grille provides approximately 2,803 mm² of total open area per corner, about 4.9 times the corresponding S6 terminus area. This increase reduces average air velocity as the flow approaches free space and gives the four S6 passages a low-restriction termination.

Figure 10 Exit Grille Area.

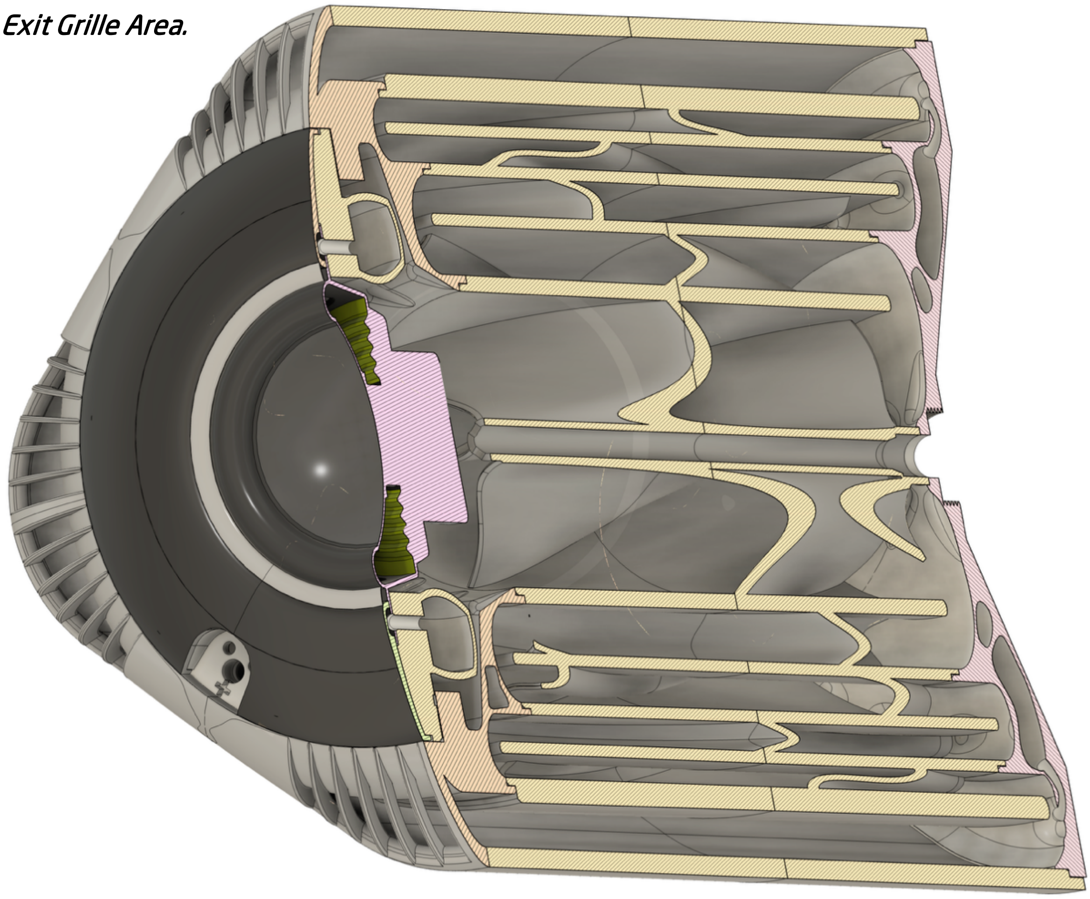

The exit grille is a permanent part of the bezel structure. Its vanes and surrounding surfaces use rounded edges throughout. Salvatti et al. (1998) found that loudspeaker-port entrance losses are strongly dependent on geometry and reported that well-rounded entrances can produce very low loss compared with sharp entrances. Because loudspeaker airflow reverses direction every half-cycle, both ends of an acoustic passage function alternately as entrances and benefit from rounded geometry.

The upper boundary of the grille entry is stepped so that the terminal expansion occurs in stages between the S6 end and the full grille area. This is illustrated in Figure 11.4.9 tlll This reduces the severity of the local adverse pressure gradient produced as the passage diverges. Salvatti et al. (1998) describe how a diverging passage causes velocity to decrease and static pressure to rise along the wall. If the expansion is too severe, the boundary layer can lose sufficient momentum for local flow reversal and separation to occur. They consequently identify a more gradual flare as preferable on the outward-flow stroke because it limits the adverse pressure gradient. The stepped Flow/2 exit geometry applies that principle by distributing the total area increase over several smaller geometric transitions.

Figure 11 Exit Grille Steps.

During inward flow, the same rounded grille openings and stepped transition provide a progressively contracting entry path toward S6. During outward flow, the expanding chamber, stepped upper surface, rounded grille vanes, and large open area reduce local velocity and pressure change as the air approaches the exterior. The geometry therefore addresses the two principal mechanisms identified in the port literature: entrance loss associated with sharp edges and boundary-layer separation associated with excessive adverse pressure gradients. Salvatti et al. further note that separated flow can form vortices that dissipate acoustic energy and contribute to compression at high drive levels.

The resulting exit structure combines a large free area, rounded surfaces, staged area increase, and fixed structural alignment. These features are expected to reduce the likelihood that the grille region will become a significant source of turbulence, compression, or audible flow noise within the intended operating range.

How Well Does It Work?

The completed Flow/2 will be compared with an existing Flow/1 control. Both enclosures include dimples, pimples, and clefts; Flow/2 adds gyroidic vanes and Helmholtz resonators. The same Dayton Audio ND91-8 driver, electronics, input level, microphone, and measurement geometry will be used for both enclosures.

Electrical impedance will be compared with the driver's free-air impedance curve to identify enclosure-related structure.

Verification will include near-field measurements of the driver response, each terminus response, summed acoustic response, phase, and decay near 149, 239, 335, and 432 Hz

(Keele, 1974). Modal peak level, bandwidth, impedance structure, phase rotation, and decay time will be reported relative to the Flow/1 control.

This section reports design objectives and calculated starting points. Measured Flow/2 fold reflection, grille radiation impedance, modal Q, and decay results will follow after the printed enclosure, resonators, and grille have been completed and tested.

Final Thoughts

Flow/2 began with a simple packaging problem: fit a tapered quarter-wave line approaching two meters in length into a compact loudspeaker enclosure and preserve the useful acoustic behavior of that line. The resulting folded, coaxial geometry resolved the packaging problem and defined the acoustic work that followed.

Six unequal-length tapered segments spread the frequencies associated with individual passage lengths. Gyroidic-like vanes vary the internal geometry from S1 through S5. Dimples, pimples, and clefts alter reflection surfaces at selected folds and transitions. Seven Helmholtz resonators provide frequency-selective treatment at calculated pressure maxima near 149, 239, 335, and 432 Hz.

The folds maintain approximately continuous net line area as the acoustic path changes direction, including the division from annular S5 into four S6 corner passages. Airflow calculations show margin through the early folds at the Dayton Audio ND91-8’s selected excursion condition and identify F5 and S6 as the highest-velocity regions near the first line mode. The four S6 passages terminate through a large, rounded, stepped exit grille whose open area reduces final air velocity.

Together, these features form a single acoustic line whose geometry provides the primary means of controlling its internal behavior. Measurements of the completed Flow/2 will determine how closely the physical loudspeaker follows these calculated design objectives.

Glossary and Acronyms

Acoustic impedance

The complex ratio of acoustic pressure to volume velocity at a specified location and frequency:

$$Z_a = \frac{p}{U}$$

Acoustic impedance is expressed in pascal-seconds per cubic meter (Pa·s/m³). Its real part represents acoustic resistance, and its imaginary part represents acoustic reactance.

Annular segment

A ring-shaped acoustic passage bounded by inner and outer surfaces around a common axis. The clear or free-flow area excludes the walls, vanes, and other solid structures occupying the passage. In Flow/2, S1 through S5 are annular segments; S6 divides into four corner passages.

Antinode

A location at which a specified field quantity reaches maximum amplitude in a standing-wave pattern. A pressure antinode has maximum pressure amplitude and, in an ideal lossless line, coincides with a particle-velocity node.

A(s), p(s), k, and s

These symbols belong to the one-dimensional reduced-order tube model.

$s$is the distance measured along the acoustic centerline from the driver toward the terminus.

$A(s)$is the local clear line area measured perpendicular to the local centerline.

$p(s)$is the complex acoustic-pressure amplitude at position s.

$k$is the acoustic wavenumber:

$$k = \frac{2\pi f}{c}$$

where $f$is frequency and $c$is the speed of sound.

The reduced-order pressure equation is:

$$\frac{d}{ds}\left[A(s)\frac{dp(s)}{ds}\right] + k^2 A(s)p(s) = 0$$

This is a one-dimensional form of Webster’s horn equation for a slowly varying tube (Rienstra, 2005; Stinson, 1991).

CAD

Computer-aided design: the digital modeling of a physical object or enclosure.

Coaxial

Having a common axis. In Flow/2, the primary line segments are nested coaxially, allowing a long acoustic path to occupy a compact enclosure.

Dimples, pimples, and clefts

Surface features placed at folds and transitions. Dimples are debossed, hemispherical recesses with broad rounded chamfers. Pimples are embossed, hemispherical protrusions. Clefts are rounded, chamfered grooves recessed into edges and troughs. These features are intended to reduce surface regularity and distribute reflections over different path lengths and angles.

DIY

Do-it-yourself: design, construction, and testing carried out by the builder.

DSP

Digital signal processing: the use of numerical processing to alter, control, or analyze an audio signal.

EQ

Equalization: frequency-dependent adjustment of signal level.

FCTQWT

Folded Coaxial Tapered Quarter-Wave Tube. Flow/2's folded, coaxial arrangement of tapered line segments sharing a common axis and connected by folds.

Fold

A short, direction-changing portion of the acoustic line that connects adjacent segments. In Flow/2, each fold forms an approximately constant-area passage with rounded transitions that preserve the net clear line area through the change in direction. Fold lengths contribute to the total centerline path length.

Grille

A protective open structure covering an acoustic opening. In Flow/2, the exit grilles cover the terminus openings. Their geometry forms part of the final radiation path and can affect local airflow and acoustic resistance.

Gyroidic-like vane

A twisted internal vane with continuously changing surfaces inspired by gyroid geometry. The term "like" indicates an approximate form. In Flow/2, the vanes connect the inner and outer walls of S1 through S5, alter the local passage geometry, add structural support, and interrupt direct line-of-sight through the segments.

Helmholtz resonator

A tuned side branch consisting of an enclosed air cavity connected to an acoustic passage through a narrow neck. The air in the neck behaves as an acoustic mass, and the compressibility of the air in the cavity provides acoustic compliance, or springiness. Together, they form a resonant system. In Flow/2, the resonators are positioned near calculated pressure antinodes to divert energy from selected higher-order tube modes. Losses dissipate part of that energy.

Modal quality factor, Q_m

A dimensionless measure of resonance sharpness and persistence. A high-Q_m mode has a narrow response and decays slowly. A low-Q_m mode has a broader response and decays more quickly.

Particle velocity

The local velocity of air particles produced by an acoustic wave. Particle velocity is a vector quantity, with both magnitude and direction, and is expressed in meters per second (m/s).

Pressure node

A location at which acoustic pressure amplitude reaches a minimum. In an ideal lossless line, a pressure node coincides with a particle-velocity antinode. The pressure at an open terminus approaches a node.

Taper

A gradual change in clear cross-sectional line area along the acoustic centerline. Flow/2 uses a generally decreasing net line area from the driver toward the terminus. Taper affects acoustic impedance, particle velocity, and standing-wave mode shapes.

Terminus

The open end of the acoustic line through which sound leaves the tube and radiates into the room. In Flow/2, the line terminates in four S6 corner passages and their exit openings.

U_{pk}

Peak driver volume velocity used in the airflow calculation. For sinusoidal driver motion:

$$U_{\mathrm{pk}} = S_d\, 2\pi f X$$

Volume velocity

The rate at which air volume passes through a cross-section of the acoustic line. It is expressed in cubic meters per second (m^3/s) or liters per second (L/s). In the airflow calculation, U_{mk} denotes peak driver volume velocity.

where $S_d$is the effective piston area of the driver, f is frequency, and $X$is peak diaphragm displacement. The quantities must use consistent units.

S1–S6

Labels for Flow/2's six acoustic line segments, ordered from the driver toward the terminus. S6 divides into four separate corner passages.

S_d

The effective piston area of the driver.

TQWT

Tapered Quarter-Wave Tube. A loudspeaker enclosure in which the driver excites a tapered acoustic line whose effective length is approximately one quarter wavelength at its first line resonance.

Xmax

The manufacturer's specified maximum linear one-way excursion of the driver diaphragm or voice coil.

Disclaimer

This document describes the theory, calculations, engineering rationale, and predicted acoustic behavior of the Flow/2 loudspeaker system. It is provided for informational and educational purposes. Calculated frequencies, pressure distributions, airflow velocities, resonator behavior, modal responses, and other predicted results are based on the models, dimensions, assumptions, and reference data described in the document. Actual performance will depend on the completed physical geometry, materials, manufacturing tolerances, driver characteristics, assembly, operating conditions, and measurement environment.

Acoustic models and calculations are approximations to physical behavior. Three-dimensional effects, viscous and thermal losses, structural vibration, nonlinear driver behavior, flow separation, radiation impedance, printing tolerances, and other physical effects may cause measured results to differ from calculated values. Predictions identified in this document remain subject to verification by measurement of the completed Flow/2 system.

adhocspeakers.com makes no guarantee that a constructed Flow/2 loudspeaker will achieve any particular acoustic response, output level, distortion level, modal attenuation, airflow behavior, or other performance characteristic described or predicted in this document. Anyone using the information presented here for analysis, modification, construction, testing, or operation of a loudspeaker system assumes responsibility for evaluating its suitability, safety, and performance.

Acknowledgements

Technical and Editorial Assistance

ChatGPT, developed by OpenAI, provided assistance with analysis of the Flow/2 acoustic and mechanical models, calculations, review of technical references, development and verification of equations and tables, measurement planning, figure preparation, and editorial refinement. The Flow concepts, inventions, CAD models, physical prototypes, measurements, design decisions, and final editorial judgments remain those of the author.

References

Augspurger, G. L. (2000). Loudspeakers on damped pipes. *Journal of the Audio Engineering Society, 48*(5), 424–436.

Bezzola, A., Devantier, A., & McMullin, E. (2019). Loudspeaker port design for optimal performance and listening experience (AES Convention Paper No. 10311). Audio Engineering Society.

Bezzola, A., Kubota, G. S., & Devantier, A. O. (2020). Acoustic mass and resistance as function of drive level for straight, bent, and flared loudspeaker ports (AES Convention Paper No. 10423). Audio Engineering Society.

Blevins, R. D. (1979). *Formulas for natural frequency and mode shape*. Van Nostrand Reinhold Company.

Bouvier, P. M. (2011). *Folded coaxial transmission line loudspeaker* (U.S. Patent No. 7,925,036 B2). U.S. Patent and Trademark Office.

Dayton Audio. (n.d.). *ND91-8 3-1/2" aluminum cone full-range driver 8 ohm*. Retrieved September 9, 2026, from https://www.daytonaudio.com/product/1045/nd91-8-3-1-2-aluminum-cone-full-range-driver-8-ohm

Guimarães, G. P., & Ribeiro, I. T. (2018). Experimental investigation on the acoustic impedance of Helmholtz resonators using an accelerometer for the volume velocity source. In *Proceedings of ISMA2018 and USD2018* (pp. 1479–1486). https://past.isma-isaac.be/downloads/isma2018/proceedings/Contribution_161_proceeding_3.pdf

Jackson, C. M. (2005). Finite-difference, time-domain analysis of a folded acoustic transmission line. *IEEE Transactions on Ultrasonics, Ferroelectrics, and Frequency Control, 52*(3), 371–378.

Keele, D. B., Jr. (1974). Low-frequency loudspeaker assessment by nearfield sound-pressure measurement. *Journal of the Audio Engineering Society, 22*(3), 154–162.

King, M. J. (2002, July 17). *Quarter wavelength loudspeaker design*. https://www.quarter-wave.com/

King, M. J. (2006). *Anatomy of a transmission line loudspeaker*. https://www.quarter-wave.com/TLs/TL_Anatomy.pdf

King, M. J. (2023, November 3). *Using modal analysis to understand transmission line speaker enclosure response: Part 1, the basics*. https://www.quarter-wave.com/TLs/Part_1_The_Basics.pdf

Levine, H., & Schwinger, J. (1948). On the radiation of sound from an unflanged circular pipe. *Physical Review, 73*(4), 383–406. https://doi.org/10.1103/PhysRev.73.383

Li, J., An, X., & Gea, H. C. (2026). Systematic design of side-branch resonators for targeted noise reduction using an ASPMSS analytical model. *Acta Acustica, 10*, Article 64. https://doi.org/10.1051/aacus/2026064

Lloyd, R. M. (1968). *Optimum placement of Helmholtz resonators for damping pressure oscillations* [Master's thesis, Princeton University]. U.S. Naval Postgraduate School. https://archive.org/download/optimumplacement00lloy/optimumplacement00lloy.pdf

Papadakis, N. M., & Stavroulakis, G. E. (2023). Tunable Helmholtz resonators using multiple necks. *Micromachines, 14*(10), 1932. https://doi.org/10.3390/mi14101932

Rapoport, Z., & Devantier, A. (2004). Analysis and modeling of the bi-directional fluid flow in loudspeaker ports (AES Convention Paper No. 6194). Audio Engineering Society.

Rienstra, S. W. (2005). Webster's horn equation revisited. *SIAM Journal on Applied Mathematics, 65*(6), 1981–2004. https://doi.org/10.1137/S0036139902413040

Salvatti, A., Button, D., & Devantier, A. (1998). Maximizing performance from loudspeaker ports (AES Preprint No. 4855). Audio Engineering Society.

Selamet, A., & Ji, Z. L. (2000). Circular asymmetric Helmholtz resonators. *The Journal of the Acoustical Society of America, 107*(5), 2360–2369. https://doi.org/10.1121/1.428622

Stinson, M. R. (1991). The propagation of plane sound waves in narrow and wide circular tubes, and generalization to uniform tubes of arbitrary cross-sectional shape. *The Journal of the Acoustical Society of America, 89*(2), 550–558. https://doi.org/10.1121/1.400379

